Dyes and Pigments 87 (2010) 139–143

Contents lists available at ScienceDirect

Dyes and Pigments

journal homepage: www.elsevier.com/locate/dyepig

Photoinduced electron transfer (PET) within D_4–A and D–A photosynthetic systems: Enhanced intramolecular PET achieved by increasing the number of donors

Xian-Fu Zhang*, Hongwei Zheng, Shuangming Jin, Ruiyun Wang

Chemistry Department, Hebei Normal University of Science and technology, Qinhuangdao, Hebei Province, 066004 PR China

A R T I C L E I N F O

Article history:
Received 5 December 2009
Received in revised form
6 March 2010
Accepted 8 March 2010
Available online 17 March 2010

Keywords:
Photoinduced electron transfer
Phthalocyanine
Phenothiazine
Charge separation
Synthesis
Fluorescence quenching

A B S T R A C T

Photoinduced electron transfer (PET) occurring within **D$_4$–A** was compared to that within **D–A**, in which **A** (electron acceptor) was a single zinc phthalocyanine moiety and **D** (electron donor) a phenothiazine unit, using UV–vis absorption, fluorescence emission and laser flash photolysis. **D** and **A** in both models were directly linked by covalent C–N bonds. The symmetrical **D$_4$–A** system, for which both the synthesis and purification were more straigthforward than for **D–A**, displayed a much faster PET rate constant; although the **D–A** system was more difficult to prepare, it exhibited less efficient PET. The charge separation state formed through PET showed long lifetimes on the μs scale in the cases of both the **D$_4$–A** and **D–A** molecules.

1. Introduction

Photoinduced electron transfer (PET) in molecular systems, that contain both electron donors (**D**'s) and acceptors (**A**'s) tethered together using various types of bridge, has been extensively explored both experimentally and theoretically [1–9]. The dominant models reported have been linearly linked $D–A_1–A_2–\cdots–A_n$ ($n \geq 1$), so that in each consecutive step of PET only one-donor-one acceptor is involved. Although papers that deal with multi-donor-one-acceptor systems (D_n–A) are rare, such D_n–A ($n > 1$) models may reveal novel features that do not occur in the more common D–A system, such as the formation of multi-charge, separated states (MCSS) $(D^{\bullet+})_k–A^{k-}$ ($k > 1$) [10–12]. MCSS can provide stronger reducing or oxidizing species than $D^{\bullet+}–A^{\bullet-}$ systems for artificial photosynthesis to reduce CO_2 and split water into dioxygen. Such reduction or water splitting requires multi reducing or oxidizing equivalents in natural photosynthesis [1,13], which is cannot be achieved using $D^{\bullet+}–A^{\bullet-}$ in artificial photosynthesis. Other than MCSS, our understanding of PET within D_n–A remains limited, especially as there is no specific understanding of how both the rate and efficiency of PET within D_n–A can be increased or decreased relative to that of the corresponding D–A. A comparative investigation of PET within a D_n–A compared to that of its corresponding D–A system is necessary to reveal such differences, but this remains an unexplored aspect of intramolecular PET. This was the purpose of this study insofar as a **D$_4$–A** model (Fig. 1) was compared to that of the corresponding **D–A** system. It is known that PET can occur in a **D$_4$–A** system [12] but this was not compared with that of the corresponding **D–A** system.

In a **D$_4$–A** supramolecule there is only one entity, namely **A**, that can accept electrons, but there are four equal donors which will concurrently donate an electron to the same acceptor **A** during the lifetime of the photo excited ZnPc. If the acceptor is allowed to hold only one electron, competition occurs between the four donors. In the case of intermolecular PET, it is well known that the greater the number of donors, the faster is PET, as effective collisions between donors and acceptors are increased. Intra-molecular PET, however, proceeds through bonding or space that involves no collisions. In general, a one–one linking of D–A can make PET occur more effectively; moreover, the direction of electron movement from any D to A in the symmetrical D_4–A system is against that on the opposite side (Fig. 1 right), which can result in the canceling out or slowing down of PET. In this work, however, it was found that PET within the D_4–A was significantly faster than that in the D–A.

---

* Corresponding author. Tel./fax: +86 0335 2039067.
E-mail address: zhangxianfu@tsinghua.org.cn (X.-F. Zhang).

0143-7208/$ – see front matter © 2010 Elsevier Ltd. All rights reserved.
doi:10.1016/j.dyepig.2010.03.010

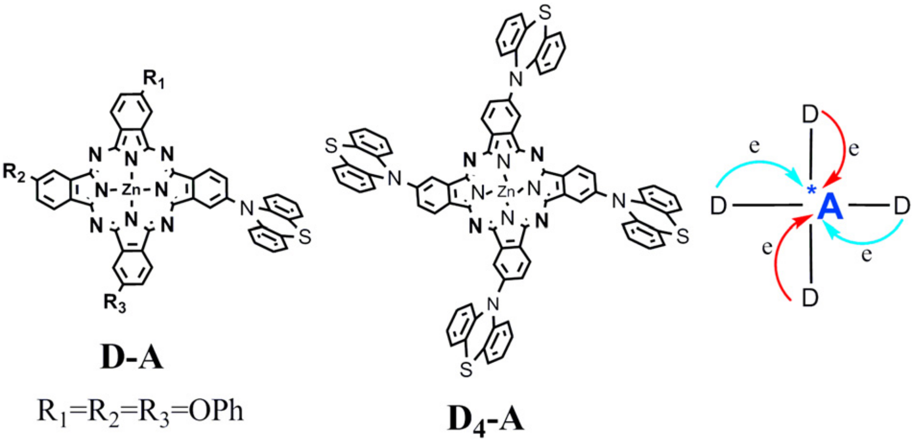

Fig. 1. Structures of D–A and D$_4$–A. D–A is produced together with D$_i$–A (i = 0, 2–4) that needs to be separated out.

ZnPc can function as a good electron acceptor and has been employed in many D–A systems [14–20], its electrochemistry and absorption spectrum of ZnPc$^{\bullet-}$ having been well documented. PTZ is a nonplanar molecule in which the two benzene rings form an angle of 140° [21]. PTZ tends to form stable PTZ$^{\bullet+}$, which is an almost coplanar system (the dihedral angle is 176.5°) so that the positive charge is delocalized [22]. The PTZ radical cation has also been well-characterized using UV–Vis methods [23–25].

2. Experimental

2.1. Materials and instruments for synthesis

All organic solvents were dried by appropriate methods and distilled before use. ZnPc was purchased from Tokyo Kaise. 4-phenoxy phthalonitrile and Tetra(β-phenoxy) zinc phthalocyanine were prepared previously by the current authors [26]. The synthesis and characterization of Tetra(β-Phenothiazinyl) zinc phthalocyanine was undertaken according to [27]. All other reagents were analytical grade and were used as received. ^{1}H NMR spectra were recorded at room temperature on a Bruker dmx 300 MHz NMR spectrometer. MS spectra were recorded either on a Bruker APEX II or Autoflex III Maldi-TOF spectrometer. IR spectra were recorded at room temperature on a Shimadzu FTIR-8900 spectrometer. Samples for C, H, N elemental analysis were dried under vacuum, and analyzed with a Carlo Erba-1106 instrument.

2.2. Preparation of 4-phenothiazinyl phthalonitrile

The procedure is based on that reported in [27]. A mixture of 4-nitrophthalonitrile (1.04 g, 6 mmol) and phenothiazine (1.20 g, 6 mmol) was stirred in dry DMSO (20 mL) under argon for 64 h at room temperature, during which time, dry potassium carbonate (2.5 g, 18.1 mmol) was added in four equal portions over 2 h. The reaction process was monitored using flash chromatography employing dichloromethane as mobile phase. After reaction was complete, the resulting solution was poured into 150 mL ice-water and filtered. The ensuing solid was washed with cold deionized water until pH was neutral, washed with cold ethanol, diethyl ether and then dried. The crude product was recrystallized twice with ethanol as solvent, which yielded yellow crystals. Yield: 54%. m.p.: 198–200 °C. MS: $m/z = 326.2$ [M + 1]$^+$. ^{1}H NMR (300 MHZ, CD_2Cl_2, 22 °C): δ 7.61–7.15 (m, 11 H, Ar-H). IR [(KBr) ν_{max}/cm^{-1}]: 3062 (Ar-H), 2222 (C≡N), 1600, 1578, 1546, 1458, 1331, 1258, 1095, 1030, 876, 825.

2.3. Preparation of β-phenothiazinyl-tri(β-phenoxy) zinc phthalocyanine

A mixture of 4-phenothiazinyl phthalonitrile (0.152 g, 0.45 mmol), 4-phenoxy phthalonitrile (0.30 g, 1.36 mmol), zinc acetate dihydrate (0.087 g, 0.40 mmol), two drops of DBU as catalyst and dry quinoline (15 ml) was heated under an argon atmosphere, with stirring, at 190 °C for 5 h. The majority of quinoline was removed by distillation under vacuum and the resulting precipitate was filtered and washed with n-hexane and then refluxed with ethanol (20 mL) and filtered to remove all traces of quinoline. The green dry product was purified by column chromatography using CH_2Cl_2–THF (v/v 19:1) as eluent. Yield: (14%). IR ν_{max}/cm^{-1}: 3063, 1616, 1589, 1485, 1369, 1312, 1277, 1234, 1092, 1041, 930, 868, 744, 694. MS (Maldi-TOF): 1050.2 [M + 1]$^+$. ^{1}H NMR ($CDCl_3$, 22 °C): δ 6.80–6.90 (m, 1H), 7.05–7.15 (d, 6H), 7.20–7.30(t, 7H), 7.30–7.35(s, 4H), 7.35–7.38(m, 2H), 7.39–7.45(t, 6H), 7.45–7.50 (d, 2H), 7.60–7.65(d, 1H), 7.80–7.85(d, 3H), 7.90–8.20(s, 3H). Anal. calcd. for $C_{62}H_{35}N_9O_3SZn$ (MW, 1049.2); C, 70.82; H, 3.36; N, 11.99. Found: C, 70.36; H, 2.98; N, 11.74.

2.4. Photophysical measurements

DMF and other solvents were dried and freshly distilled before use. Measurements were carried out at room temperature of 22 °C. UV–vis absorption measurements were made with an HP 8451A or Shimadzu 4500 spectrophotometer in 10 mm quartz cuvettes. Fluorescence spectra up to 900 nm were monitored using a PerkinElmer LS 55, with 2.5 nm slits. All spectra were corrected for the sensitivity of the photo-multiplier tube. The fluorescence quantum yield (Φ_f) was calculated by $\Phi_f = F_s A_0 \Phi^0{}_f/(F_0 A_s)$, in which F is the integrated fluorescence intensity, A is the absorbance at excitation wavelength, the subscript 0 stands for a reference compound and s represents samples. Zinc phthalocyanine in DMF was used as the reference ($\Phi^0{}_f = 0.30$) [28]. Excitation wavelengths of 610 nm corresponding to S_0 to S_1 transitions were employed. The sample and reference solutions were prepared with the same absorbance (Ai) at the excitation wavelength (near 0.09 per cm). All solutions were air saturated. Fluorescence lifetime of S_1 was measured by time-correlated single photon counting method (Edinburgh FL-900 spectrophotometer) with excitation at 660 nm by a CdS portable diode laser (50 ps) and emission was monitored at 700 nm. Transient spectra were recorded in degassed DMF (prepared by bubbling with Argon for 20 min) with an Edinburgh LP-920 laser flash photolysis system. A Nd:YAG laser (Continuum surelite II, 355 nm and 7 ns FWHM) was used as excitation source. The analyzing light was from a xenon lamp. The laser and analyzing light beams perpendicularly passed through a quartz cell with an optical path length of 1 cm. The signal was displayed and recorded on a Tektronix TDS 3012B oscilloscope and an Edinburgh LP900 detector. The laser energy incident at the sample was attenuated to a few mJ per pulse. Time profiles at a series of wavelengths from which point by-point spectra were assembled were recorded with the aid of a PC controlled kinetic absorption spectrometer. The concentrations of the target compounds were typically 10 μM providing $A_{355} = 0.3$ in a 10 mm cuvette.

3. Results and discussion

The attachment of a single PTZ entity to ZnPc is of the asymmetrical synthesis and was accomplished by the common cross condensation method [29], as shown in Fig. 2. The formation of additional D_i–A ($i = 0$ to 4 but not 3) lowers the yield and increases isolation difficulty. A D_4–A, on the other hand, can be prepared by the symmetrical method without worrying about the formation of other D_i–A ($i = 0$–3) [30].

The electronic absorption spectra are given in Fig. 3. Comparing the spectra with that of ZnPc(β-OPh)$_4$ i.e., tetra(β-phenoxy) ZnPc, it is clear that the long wavelength Q band of **D**–**A** or **D$_4$**–**A** corresponds essentially to that of the ZnPC moiety, i.e., **A** itself. This is owing to the very small π-electronic interaction between the two moieties **D** and **A** at ground state caused by the sterically favored orthogonal orientation. The "extra" PTZs do not influence the electronic properties of PC moiety since the absorption spectra of D–A and D_4–A show little difference.

Also noted is the absence of the band at 630 nm attributed to the intermolecular dimer or higher aggregates formed by two or more phthalocyanines. The Beer's law is also obeyed according to the obtained linear relation between absorbance and the concentration of **D**–**A** or **D$_4$**–**A** up to 10 μM, which further removes the possibility of aggregation effect upon photophysics.

The fluorescence emission spectra in DMF measured by exciting PC moieties at 610 nm are compared in the inset of Fig. 4. With photoexcitation under the same conditions, the emission intensities are remarkably different between the four compounds. **D$_4$**–**A** showed the most significant fluorescence quenching with a fluorescence quantum yield (Φ_f) of 0.040. The Φ_f of **D**–**A** is 0.080, which is 2-fold of that of **D$_4$**–**A**. ZnPc(β-OPh)$_4$, the model compound of **A**,

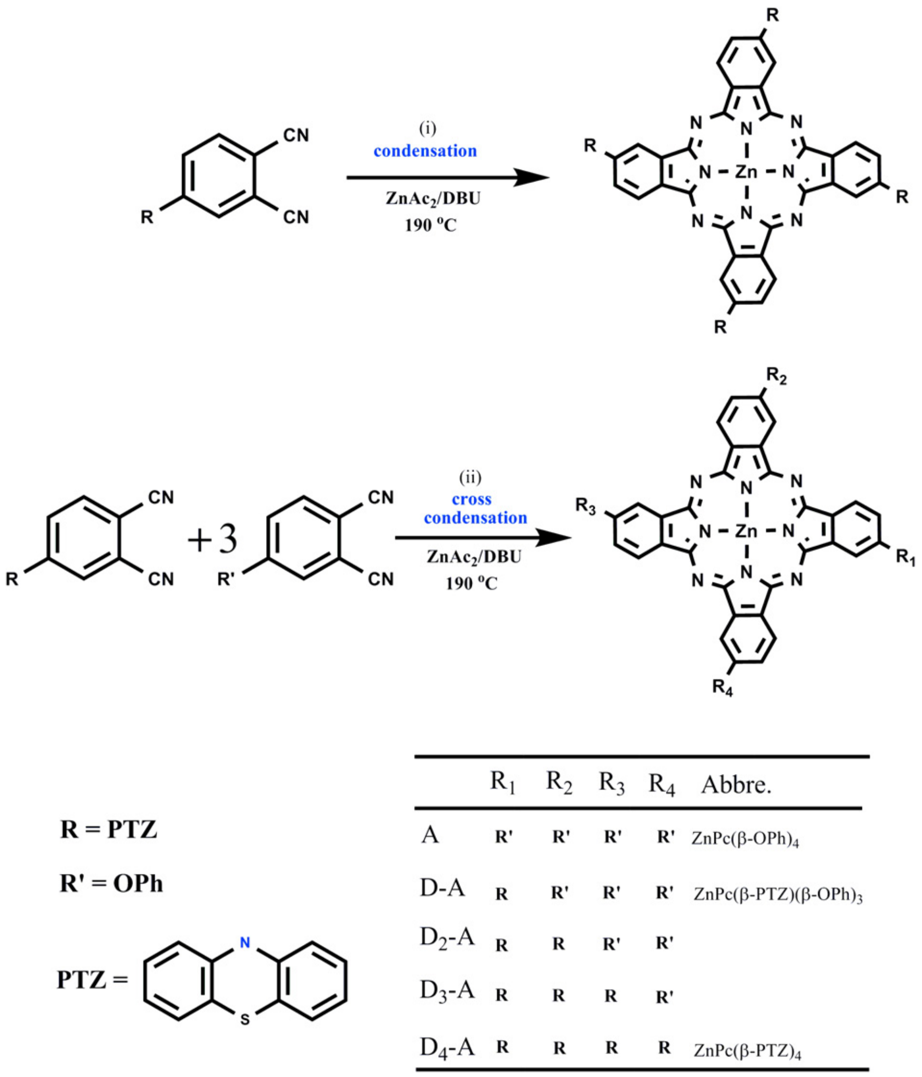

R = PTZ

R' = OPh

PTZ =

	R$_1$	R$_2$	R$_3$	R$_4$	Abbre.
A	R'	R'	R'	R'	ZnPc(β-OPh)$_4$
D-A	R	R'	R'	R'	ZnPc(β-PTZ)(β-OPh)$_3$
D$_2$-A	R	R	R'	R'	
D$_3$-A	R	R	R	R'	
D$_4$-A	R	R	R	R	ZnPc(β-PTZ)$_4$

Fig. 2. The comparison of symmetrical and asymmetrical synthesis for D_4–A and D–A, respectively.

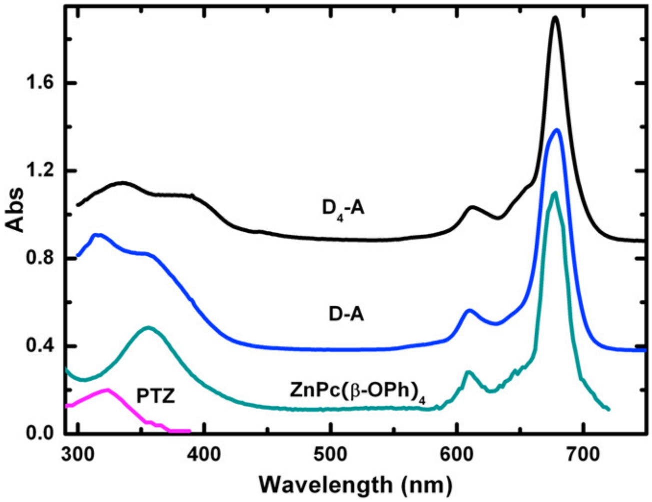

Fig. 3. UV–Vis absorption spectra of PTZ, D–A, D_4–A and ZnPc(β-OPh)$_4$ in DMF solutions. The latter three spectra were raised for clear viewing.

exhibited only a slight decrease of emission intensity ($\Phi_f = 0.26$) from that of ZnPc ($\Phi_f = 0.30$).

The fluorescence decays (Fig. 4) were monitored at 700 nm with laser excitation at 660 nm. The emission of both ZnPc and ZnPc(β-OPh)$_4$ decays mono exponentially with slightly different lifetime (τ_f) of 3.54 ns and 3.47 ns, respectively. The decay kinetics of **D**–**A** and **D$_4$**–**A**, however, is biexponential. τ_f of **D$_4$**–**A** is 0.39 ns (74.6%) and 3.69 ns (25.4%), while that for **D**–**A** is 1.45 ns (95.4%) and 3.20 ns (4.6%), respectively. The long-lived but minor components are usually attributed to the conformers unfavoring PET. The τ_f of the major but short-lived component of D_4–A was significantly reduced to 0.39 ns from 1.45 ns that in the D–A dyad, while the latter was also decreased from 3.47 ns of ZnPc(β-OPh)$_4$.

It is clear that the singlet excited state (S_1) of ZnPc moiety within both D–A and D_4–A is efficiently quenched by the occurrence of PTZ, and the number of PTZ moieties showed remarkable effect on the quenching efficiency. The enhancement of internal conversion (IC) by PTZs can be excluded, since ZnPc(β-OPh)$_4$ that possess faster rotational and vibrational OPh groups than phenothiazinyl showed only a slight decreased Φ_f and τ_f compared with that of ZnPc. The energy transfer from ZnPc moiety to PTZ is not possible because PTZ does not absorb in the red region. This quenching must be owing to the PET from PTZ to S_1 of ZnPc within the **D**–**A** and **D$_4$**–**A**, which is also indicated from the thermodynamic and transient absorption studies below.

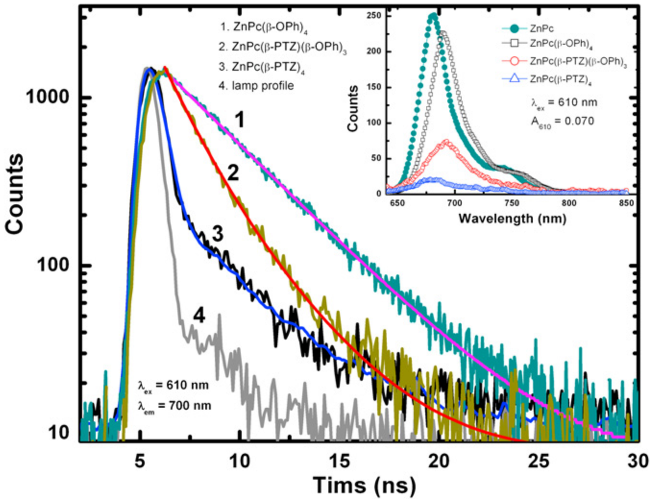

Fig. 4. Steady state (inset) and dynamic fluorescence quenching of ZnPc moiety by the substitution of PTZ in DMF. The excitation wavelength for steady state fluorescence is 610 nm (Xenon lamp), the fluorescence decay was measured by single photon counting method with excitation at 660 nm by diode laser (50 ps) and emission at 700 nm. The values of χ^2 for the fitting are between 1.10 and 1.25.

The rate constant of PET (k_{et}) value can be calculated from the fluorescence lifetime using $k_{et} = (\tau_f)^{-1} - (\tau^0{}_f)^{-1}$. PET within **D$_4$**–**A** occurred with $k_{et} = 2.28 \times 10^9\ s^{-1}$, which is about five times faster than that in **D**–**A** ($k_{et} = 0.43 \times 10^9\ s^{-1}$). The efficiency of PET within **D$_4$**–**A** is 0.90, calculated by $(\Phi^0{}_f/\Phi_f - 1)/\tau^0{}_f$, which is 1.5 times larger than that of the D–A (0.60).

Both phthalocyanies and PTZ's redox properties have been extensively studied. The oxidation potential of PTZ appeared at $E_{(PTZ/PTZ^{\bullet +})} = 0.73$ V (vs SCE) and the reduction potential occurred at −2.20 V [31], while ZnPc exhibited reduction peak at $E_{(ZnPc^{\bullet -}/ZnPc)} = -0.83$ V and oxidation peak at 0.86 V in DMF [32]. PTZ is obviously easier to be oxidized than ZnPc according to their redox potentials. PET from PTZ to S_1 of ZnPc moiety is thermodynamically favored, since its ΔG is a negative value obtained by: $\Delta G_{PET} = E_{(PTZ/PTZ^{\bullet +})} - E_{(ZnPc^{\bullet -}/ZnPc)} - E_{00} - 0.06 = 0.73 - (-0.83) - 1.84 - 0.06 = -0.34$ eV. PET by the photo excitation of PTZ is even more favored, since $\Delta G_{PET} = 0.73 - (-0.83) - 3.22 - 0.06 = -1.72$ eV, which is much more negative. In practice, however, the light illumination in UV region mainly populates the S_2 state of ZnPc moiety rather than S_1 of PTZ, because the former possesses a much larger ε, especially in the region above 350 nm. Unlike the previous system in which the double electron transfer from two donors to the same S_2 of ZnPc moiety is feasible [12], the same process is not possible within the current D_4–A, because the associated ΔG_{PET} is a positive value of 0.26 eV. Also noted is the electron transfer between **D** and **A** without photoexcitation is not allowed owing to $\Delta G_{ET} = E_{ox} - E_{red} - C = 0.73 - (-0.83) - 0.06 = 1.50$ eV. PET from PTZ to T_1 of ZnPc moiety is also forbidden, since the energy of the T_1 state is 0.99 eV [33,34], suggesting a ΔG_{PET} of +0.51 eV. In conclusion, based on the thermodynamic analysis, only single electron can be transferred from PTZ to S_1 of ZnPc moiety within both **D**–**A** and **D$_4$**–**A**, hence the competition occurs in the D_4–A between donors for PET.

The occurrence of radical ions generated by PET was confirmed by the transient absorption spectra measured under the same conditions. In accordance with the well-known triplet–triplet excited-state absorption (T_1–T_n) of ZnPc [33,34], we found a broad

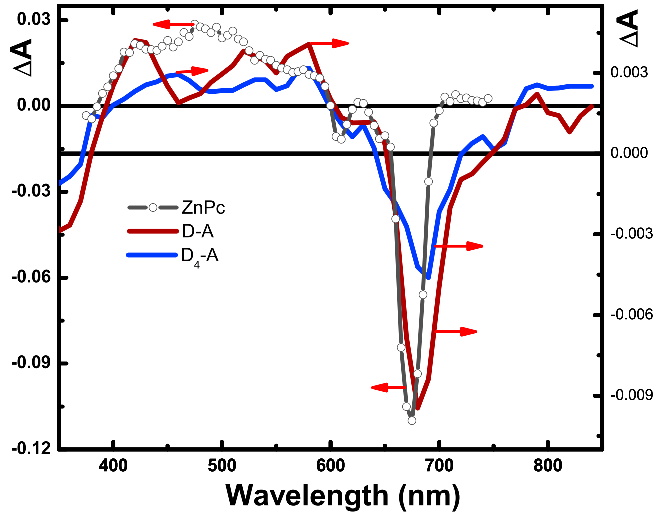

Fig. 5. Transient absorption spectra of ZnPc, D–A and D_4–A (5 µs delay) in argon saturated DMF with excitation at 355 nm (absorbance ∼0.30, laser energy ∼3 mJ) by Nd:YAG laser.

absorption band peaking around 480 nm in the spectral region around 400–630 nm for ZnPc reference compound, Fig. 5. The monoexponential decay at 480 nm gave the T_1 lifetime of 200 μs. New bands occurred at 420 nm, 530 nm and 570 nm etc. upon the laser pulse excitation (355 nm) of a deaerated DMF solution of either D–A or D_4–A as shown in Fig. 4. The most obvious is the band at 570 nm and the one above 800 nm owing to anion radical $A^{\bullet -}(ZnPc^{\bullet -})$ [35]. The 630 nm band of anion radical was weakened but still resolvable because it overlaps with the bleaching of ZnPc's ground state. A large number of studies are available for the generation and recording of anion radicals of metal phthalocyanines, $ZnPc^{\bullet -}$ is known to have major absorptions at 570, 630, and above 800 nm [35]. The monoexponential decay at 570 nm exhibits a lifetime of $\tau_d = 4.9$ μs, which is expected to reflect the back electron transfer process, for that we obtained a rate constant ($k_{BET} = 1/\tau_d$) of $2.04 \times 10^5\ s^{-1}$. The PTZ cation has long been reported to exhibit broad absorptions with maximum at 530 nm, 420 nm [23–25]. The two bands are superimposed with that of ZnPc triplet but still resolvable. The overall transient absorbance of D–A is ten times weaker than that of ZnPc, owing to the reduced formation of T_1 via ISC from S_1, another indication of a very competitive PET process from S_1. The transient absorption for D_4–A is further weakened in comparison with that of D–A, which affords another support that the more the donors, the faster the PET.

4. Conclusion

In conclusion, we explored the difference of PET between D_4–A and D–A models. The effect of the number of donors on the rate constant and efficiency of intramolecular PET is an aspect rarely discussed before. We showed that PET within **D_4–A** is more than five times faster than that in **D–A**. More over, **D_4–A** is significantly easier to be synthesized and purified than its **D–A** counterpart. Together with the previous report that a double-charge separated state $(D^{\bullet +})_2$–A^{2-} can be formed [12] in the model by selecting **D** or **A**, we believe that a multi-donor one acceptor model **D_4–A** can provide opportunity for more efficient photosynthesis mimicking.

References

[1] Barber J. Chem Soc Rev 2009;38:185–96.
[2] Liu JY, Ermilov EA, R der B, Ng DKP. Chem Commun; 2009:1517–9.
[3] Gei B, Lambert C. Chem Commun; 2009:1670–2.
[4] Medina A, Claessens CG, Rahman GMA, Lamsabhi AM, Mó O, Yá ez M, et al. Chem Commun; 2008:1759–61.
[5] Qvortrup K, Bond AD, Nielsen A, McKenzie CJ, Kils K, Nielsen MB. Chem Commun; 2008:1986–8.
[6] Deng W, Onji T, Yamaguchi H, Ikeda N, Harada A. Chem Commun; 2006: 4212–4.
[7] Hasobe T, Sandanayaka ASD, Wada T, Araki Y. Chem Commun; 2008: 3372–4.
[8] Li Y, Cao L, Tian H. J Org Chem 2006;71:8279–82.
[9] Sun S, Zhang R, Andersson S, Pan J, kermark B, Sun L. Chem Commun; 2006:4195–7.
[10] Zhang XF, Cui X, Liu Q, Zhang F. Phys Chem Chem Phys 2009;11:3566–72.
[11] Zhang XF, Cui X, Liu Q, Zhang F. ChemPhysChem 2008;9:1514–8.
[12] Zhang XF, Di Y, Zhang F. J Photochem Photobiol A: Chemistry 2009;203: 216–21.
[13] Dau H, Haumann M. Photosyn Res 2007;92:327–43.
[14] Kojima T, Honda T, Ohkubo K, Shiro M, Kusukawa T, Fukuda T, et al. Angew Chem Int Ed 2008;47:6712–6.
[15] Ballesteros B, de la Torre G, Ehli C, Rahman GMA, Agullo-Rueda F, Guldi DM, et al. J Am Chem Soc 2007;129:5061–8.
[16] Ito F, Ishibashi Y, Khan SR, Miyasaka H, Kameyama K, Morisue M, et al. J Phys Chem A 2006;110:12734–42.
[17] Ng ACH, Li X, Ng DKP. Macromolecules 1999;32:5292–8.
[18] Gouloumis A, de la Escosura A, Vazquez P, Torres T, Kahnt A, Guldi DM, et al. Org Lett 2006;8:5187–90.
[19] Atienza C, Martín N, Wielopolski M, Haworth N, Clark T, Guldi DM. Chem Commun; 2006:3202–4.
[20] Loi MA, Denk P, Hoppe H, Neugebauer H, Winder C, Meissner D, et al. J Mater Chem 2003;13:700–4.
[21] Bell JD, Blount JF, Briscoe OV, Freeman HC. Chem Commun (London); 1968:1656.
[22] Uchida T, Ito M, Kozawa K. Bull Chem Soc Jpn 1983;56:577–82.
[23] Sasaki Y, Araki Y, Ito O, Alam MM. Photochem Photobiol Sci 2007;6:560–5.
[24] Danielson E, Elliott CM, Merkert JW, Meyer TJ. J Am Chem Soc 1987;109: 2519–20.
[25] Klumpp T, Linsenmann M, Larson SL, Limoges BR, Bürssner D, Krissinel EB, et al. J Am Chem Soc 1999;121:1076–87.
[26] Zhang XF, Ma J, Xu H. Proc SPIE-Int Soc for Opt Eng 1993;1616:372–5.
[27] Sasmaz S, Agar E, Agar A. Dyes Pigm 1999;42:137–42.
[28] Seybold PG, Gouterman M. J Mol Spectrosc 1969;31:1–6.
[29] Rodriguez MS, Torre GDl, Torres T. In: Kadish KM, Smith KM, Guilard R, editors. The porphyrin handbook, vol. 16. Academic Press; 2003. p. 125–60.
[30] Mckeown NB. In: Kadish KM, Smith KM, Guilard R, editors. The porphyrin handbook, vol. 16. Academic Press; 2003. p. 61–124.
[31] Urasaki N, Yoshida S, Ogawa T, Kozawa K, Uchida T. Bull Chem Soc Jpn 1994;67:2024–30.
[32] L'her M, Pondaven A. In: Kadish KM, Smith KM, Guilard R, editors. The porphyrin handbook, vol. 16. Academic Press; 2003. p. 117–70.
[33] Carmichael I, Hug GL. J Phys Chem Ref Data 1986;15:1–250.
[34] Ishii K, Kobayashi N. In: Kadish KM, Smith KM, Guilard R, editors. The porphyrin handbook, vol. 16. Academic Press; 2003. p. 1–42.
[35] Mack J, Stillman M. In: Kadish KM, Smith KM, Guilard R, editors. The porphyrin handbook, vol. 16. Academic Press; 2003. p. 43–116.